Journal of Statistical Physics, Vol. 74, Nos. 3/4, 1994

Retrieval and Chaos in Extremely Diluted Q-Ising Neural Networks

D. Bollé,[1,2] G. M. Shim,[1] B. Vinck,[1] and V. A. Zagrebnov[1,3]

Received June 16, 1993

Using a probabilistic approach, the deterministic and the stochastic parallel dynamics of a Q-Ising neural network are studied at finite Q and in the limit $Q \to \infty$. Exact evolution equations are presented for the first time-step. These formulas constitute recursion relations for the parallel dynamics of the extremely diluted asymmetric versions of these networks. An explicit analysis of the retrieval properties is carried out in terms of the gain parameter, the loading capacity, and the temperature. The results for the $Q \to \infty$ network are compared with those for the $Q=3$ and $Q=4$ models. Possible chaotic microscopic behavior is studied using the time evolution of the distance between two network configurations. For arbitrary finite Q the retrieval regime is always chaotic. In the limit $Q \to \infty$ the network exhibits a dynamical transition toward chaos.

KEY WORDS: Graded-response networks; parallel dynamics; extreme dilution; chaotic behavior; probabilistic approach.

1. INTRODUCTION

In a recent paper[1] we have studied the parallel dynamics of extremely diluted asymmetric Q-state Potts and Q-Ising neural networks using a probabilistic approach. (For an extensive list of references on Q-state networks we refer to that paper.) This dynamics has been solved explicitly for $Q=3$. In particular, the dynamical capacity–temperature diagram and the temperature dependence of the relevant order parameters have been

[1] Instituut voor Theoretische Fysica and Interdisciplinair Centrum voor Neurale Netwerken, K.U. Leuven, B-3001 Leuven, Belgium.

[2] e-mail: FGBDA18@BLEKUL11.BITNET.

[3] On leave of absence from the Laboratory of Theoretical Physics, Joint Institute for Nuclear Research, Dubna 141980, Russia; present address: CPT, Université d'Aix-Marseille, F-13288 Marseille, Cedex 9, France.

0022-4715/94/0200-0565$07.00/0

obtained. It has been argued that, to determine the optimal retrieval quality of the Q-Ising network, one has to take into account the main overlap, the neuron activities, and the Hamming distance measuring the resemblance between the microscopic state of the network and an embedded pattern.

In the present work we extend these results to the case of analog neurons ($Q \to \infty$). Discussions on the dynamics of related networks of analog neurons in the case of extreme dilution can be found in refs. 2–5.

Furthermore, we provide a detailed comparative discussion of the macroscopic structure of the retrieval region for the $Q=3$, $Q=4$, and $Q \to \infty$ Ising models at arbitrary temperatures.

Next, we study the microscopic properties of the retrieval dynamics for these networks. Indeed, since the deterministic evolution is defined initially in the configuration space, it is natural to investigate neural networks as (discrete-time) dynamical systems. After the paper of Gardner[6] and especially after the rigorous results of Newman[7] it has become clear that for symmetric neural networks the vicinity of any stored pattern is rather complex. It contains a hierarchically structured cloud of fixed points which has a basin of attraction separating it from the clouds corresponding to the other embedded patterns. Since a detailed analysis of the attractors is complicated even in the simpler case of dynamical systems with only a few degrees of freedom (see, e.g., ref. 8), it is obvious that in a neural network with an extensive number of embedded patterns the overall structure of the clouds of attractors corresponding to different patterns is far from being clear.

In ref. 9 the simplification of the (continuous-time) dynamics due to the asymmetry of the random couplings has been used to discuss the asymptotic behavior of such a network with graded-response neurons in the vicinity of the fixed points. An extremely diluted version of this model has been considered in ref. 10. It was discovered that the time autocorrelation function of a single neuron is decaying (i.e., the evolution is mixing) in a certain region of the model parameters. Because the corresponding Lyapunov exponents are positive, this regime was called chaotic. Recently an analogous approach has been followed in ref. 11 for a fully connected network with discrete parallel updating. In this case the chaotic regime can be suppressed by introducing external noise.

In ref. 12 dynamical properties of diluted networks of analog neurons with finite-range interactions are studied. Attention is focused on the Jacobian of the nonlinear mapping defining the dynamics. Due to the randomness of the embedded patterns this Jacobian has a random nature. Using a Gaussian Ansatz, the Lyapunov exponents for the motion in the configuration space are extracted numerically from this Jacobian. It is

found that the largest Lyapunov exponent can be positive, implying that the microscopic evolution can be chaotic.

Local instability between arbitrarily close configurations has been used as a characterization of chaos in refs. 13–15 for extremely diluted binary networks, diluted asymmetric spin-glasses, and layered networks of binary neurons. The same line of reasoning has been followed for higher-order binary networks with Gaussian background noise in ref. 17. In this work we generalize this approach to Q-Ising networks and networks of graded-response neurons.

The rest of this paper is organized as follows. In Section 2 the deterministic and the stochastic dynamics of the fully connected Q-Ising neural network are defined. The Hamming distance is introduced as a macroscopic measure of the resemblance between the microscopic network state and an embedded pattern. In Section 3 the evolution equations for the overlap and the activity in extremely diluted versions of these networks are derived. An extensive analysis of the retrieval regime in the $Q=3$, $Q=4$, and $Q \to \infty$ models is given in Section 4. The results are synthesized in capacity–gain diagrams, accompanied by tables to clarify the structure of the macroscopic retrieval dynamics (attractors, repellors, saddle points). In Section 5 the microscopic properties of the retrieval dynamics are studied. Based on the exact solvability of this dynamics, an explicit analysis in terms of the Hamming distance shows that two initially close trajectories that are correlated with only one stored pattern strongly repel each other. For Q-state neurons this occurs in the whole capacity–gain plane, for graded-response neurons there exists a transition line in this plane at which the chaotic behavior sets in. This discussion is a generalization of the results of refs. 13–15 to the case of Q-Ising networks. Finally, Section 6 contains some concluding remarks.

2. THE MODEL

Consider a network Λ consisting of N neurons which can take values in a discrete set $\mathcal{S} = \{-1 = s_1 < s_2 < \cdots < s_{Q-1} < s_Q = +1\}$. The p patterns to be stored in this network, $\{\xi_i^\mu \in \mathcal{S}\}$, $i \in \Lambda = \{1, 2, \ldots, N\}$, $\mu \in \mathcal{P} = \{1, 2, \ldots, p\}$, are supposed to be independent and identically distributed random variables (i.i.d.r.v.) with zero mean, $\mathrm{E}[\xi_i^\mu] = 0$, and variance $A = \mathrm{Var}[\xi_i^\mu]$. The latter is a measure for the activity of the patterns.

Given a configuration $\boldsymbol{\sigma}_\Lambda = \{\sigma_j\}$, $j \in \Lambda$, the local field in neuron $i \in \Lambda$ is

$$h_i(\boldsymbol{\sigma}_{\Lambda \setminus i}) = \sum_{j \in \Lambda \setminus i} J_{ij} \sigma_j \tag{1}$$

where the synaptic couplings are given by

$$J_{ij}=\frac{1}{NA}\sum_{\mu\in\mathscr{P}}\xi_i^\mu\xi_j^\mu \tag{2}$$

The stochastic parallel dynamics of this network at temperature $T=\beta^{-1}$ is defined by the transition probabilities

$$\Pr\{\sigma_i(t+1)=s_k\in\mathscr{S}\,|\,\boldsymbol{\sigma}_{\Lambda\setminus i}(t)\}=\frac{\exp[-\beta\varepsilon_i(s_k|\boldsymbol{\sigma}_{\Lambda\setminus i}(t))]}{\sum_{s\in\mathscr{S}}\exp[-\beta\varepsilon_i(s|\boldsymbol{\sigma}_{\Lambda\setminus i}(t))]} \tag{3}$$

Here the energy potential $\varepsilon_i(s|\boldsymbol{\sigma})$ of neuron i is taken to be[18]

$$\varepsilon_i(s|\boldsymbol{\sigma}_{\Lambda\setminus i})=-\tfrac{1}{2}(h_i(\boldsymbol{\sigma}_{\Lambda\setminus i})\,s-bs^2),\qquad b>0 \tag{4}$$

At zero temperature the dynamics (3)–(4) at $i\in\Lambda$ takes the form

$$\sigma_i(t)\to\sigma_i(t+1)=s_k:\min_{s\in\mathscr{S}}\varepsilon_i(s|\boldsymbol{\sigma}_{\Lambda\setminus i}(t))=\varepsilon_i(s_k|\boldsymbol{\sigma}_{\Lambda\setminus i}(t)) \tag{5}$$

This rule is equivalent to using a gain function $g(\cdot)$ which has, since $\mathscr{S}$ is discrete, a steplike shape

$$\sigma_i(t+1)=g[h_i(\boldsymbol{\sigma}_{\Lambda\setminus i}(t))]$$

$$g(x)=\sum_{k=1}^{Q}s_k[\theta(b(s_k+s_{k+1})-x)-\theta(b(s_{k-1}+s_k)-x)] \tag{6}$$

where $s_0=-\infty$ and $s_{Q+1}=+\infty$. In the sequel we will restrict the discussion to the case of equidistant states such that

$$\mathscr{S}=\mathscr{S}_Q=\left\{s_k=-1+\frac{2(k-1)}{Q-1},\,k=1,2,\ldots,Q\right\} \tag{7}$$

Consequently, in the limit $Q\to\infty$, i.e., for analog neurons, the step function (6) becomes the piecewise linear function

$$g(x)=\frac{1}{2}\left[\left|\frac{x}{2b}+1\right|-\left|\frac{x}{2b}-1\right|\right] \tag{8}$$

To measure the macroscopic resemblance between the microscopic state of the network and an embedded pattern we introduce the Hamming distance

$$d_{\mathrm{H}}(\boldsymbol{\sigma}_\Lambda(t),\boldsymbol{\xi}^\nu)=\frac{1}{N}\sum_{i\in\Lambda}[\sigma_i(t)-\xi_i^\nu]^2$$

$$=\frac{1}{N}\sum_{i\in\Lambda}(\xi_i^\nu)^2+\frac{1}{N}\sum_{i\in\Lambda}[\sigma_i(t)]^2-\frac{2}{N}\sum_{i\in\Lambda}\xi_i^\nu\sigma_i(t) \tag{9}$$

This relation naturally leads to the main overlap

$$m_A^\nu(t) = \frac{1}{NA} \sum_{i \in A} \xi_i^\nu \sigma_i(t) \tag{10}$$

and the arithmetic mean of the neuron activities

$$a_A(t) = \frac{1}{N} \sum_{i \in A} (\sigma_i(t))^2 \tag{11}$$

3. EVOLUTION EQUATIONS AFTER EXTREME DILUTION

Suppose that the initial configuration $\{\sigma_i(0)\}$, $i \in A$, is a collection of i.i.d.r.v. with mean $\mathrm{E}[\sigma_i(0)] = 0$, variance $\mathrm{Var}[\sigma_i(0)] = a(0)$ and correlated with only one stored pattern:

$$\mathrm{E}[\xi_i^\mu \sigma_i(0)] = \delta_{\mu,\nu} m_0 A, \qquad m_0 > 0 \tag{12}$$

Following the analysis in ref. 1, we arrive at

$$h_i(\boldsymbol{\sigma}(0)) \equiv \lim_{N \to \infty} h_i(\boldsymbol{\sigma}_{A \setminus i}(0)) \overset{\mathscr{D}}{=} \xi_i^\nu m^\nu(0) + [\alpha a(0)]^{1/2} \mathcal{N}(0, 1) \tag{13}$$

where, as indicated, the convergence is in distribution[16] and where the quantity $\mathcal{N}(0, 1)$ is a Gaussian random variable with expectation 0 and variance 1.

This allows us to derive the first time-step in the evolution of the fully connected network. However, as explained in ref. 1, the difficulty in this type of system is the strong feedback as well as the complicated structure of the correlations. Therefore we consider the extremely diluted version of the network. The most important consequence of this fact is that the architecture of the network gets the structure of a directed tree with an average number of incoming and outgoing connections both equal to c. It is assumed that $c \ll N$. It is then justified to first dilute the system by taking the limit $N \to \infty$ and second, in the diluted system, to apply the law of large numbers (LLN) and the central limit theorem (CLT) by taking the limit $c \to \infty$.[16] The probability to have feedback in the system is zero and the correlations are now treelike. Adapting the structure of the network in this way also implies that the averages, e.g., $m^\nu(0)$ in (13), have to be taken over the treelike structure and that the loading α is redefined by $p = \alpha c$. Furthermore, $\{\sigma_i(1)\}$, $i \in \mathbb{N}$, is a collection of i.i.d.r.v. correlated with only the νth pattern, such as the $\{\sigma_i(0)\}$. Hence the first step dynamics describes the full time evolution of the network.

For zero temperature, (13) directly leads to[1]

$$a(t+1)=\int_{-\infty}^{+\infty} Dz \langle\langle g^2(\xi^\nu m^\nu(t)+[\alpha a(t)]^{1/2} z)\rangle\rangle \tag{14}$$

$$m^\mu(t+1)=\delta_{\mu,\nu}\int_{-\infty}^{+\infty} Dz \frac{1}{A}\langle\langle \xi^\nu g(\xi^\nu m^\nu(t)+[\alpha a(t)]^{1/2} z)\rangle\rangle \tag{15}$$

where $g(\cdot)$ is now an arbitrary input–output function, $\langle\langle\cdot\rangle\rangle$ denotes the average over the distribution of the patterns, and $Dz = dz[\exp(-z^2/2)]/(2\pi)^{1/2}$.

For nonzero temperatures, (13) gives, taking also the average over the temperature in the sense of (3),

$$a(t+1)=\left\langle\!\!\left\langle \int_{-\infty}^{\infty} Dz\, \overline{s^2}(\xi^\nu m^\nu(t)+[\alpha a(t)]^{1/2} z)\right\rangle\!\!\right\rangle \tag{16}$$

$$m^\mu(t+1)=\delta_{\mu,\nu}\frac{1}{A}\left\langle\!\!\left\langle \xi^\nu \int_{-\infty}^{\infty} Dz\, \bar{s}(\xi^\nu m^\nu(t)+[\alpha a(t)]^{1/2} z)\right\rangle\!\!\right\rangle \tag{17}$$

where we have introduced the notation

$$\overline{f(s)}(h)=\frac{\sum_{s\in\mathscr{S}_Q} f(s)\exp[\frac{1}{2}\beta s(h-bs)]}{\sum_{s\in\mathscr{S}_Q}\exp[\frac{1}{2}\beta s(h-bs)]} \tag{18}$$

We remark that the $\sum_{s\in\mathscr{S}_Q}$ becomes an integral over s for graded-response neurons.

4. MACRODYNAMICS: RETRIEVAL

We now discuss the information concerning the macroscopic structure of the retrieval dynamics which can be extracted by analytical and numerical methods from the fixed-point equations (14)–(17).

It is necessary to distinguish among three different types of solutions to these equations. The zero solution Z is, evidently, determined by $m=0$ as well as $a=0$. A sustained activity solution S is defined by $m=0$ but $a\neq 0$. Finally there are solutions with both $m\neq 0$ and $a\neq 0$. Nonattracting solutions of the last type are denoted by NR (for nonretrieval), attracting ones by R (for retrieval).

For the $Q=3$ system at $T=0$ we have that $\mathscr{S}_3=\{-1,0,1\}$. The explicit form of the fixed-point equations is given in ref. 1. The solution Z is stable for any value of b and α. Solutions S satisfy the equation

$$a=1-\mathrm{Erf}\left[\frac{b}{(2\alpha a)^{1/2}}\right] \tag{19}$$

where

$$\mathrm{Erf}[x] = \frac{2}{\sqrt{\pi}} \int_0^x dt\, e^{-t^2} \tag{20}$$

Their stability is determined by the sign of the eigenvalues

$$\lambda_1(a) = -1 + \frac{1}{(2\pi\alpha a)^{1/2}} \exp\left(-\frac{b^2}{2\alpha a}\right) \tag{21}$$

$$\lambda_2(a) = -1 + \frac{b}{(2\pi\alpha a^3)^{1/2}} \exp\left(-\frac{b^2}{2\alpha a}\right) \tag{22}$$

If $\alpha > \alpha_S(b) = (b/B)^2$, $B \approx 0.576$, there are two solutions to (19), which we denote by a_1 and $a_2 < a_1$. We find that $\lambda_2(a_1) < 0$ and $\lambda_2(a_2) > 0$ for any values of b and α. The values of $\lambda_1(a_1)$ and $\lambda_1(a_2)$ depend on b and α changing the stability of $S_1 = (0, a_1)$ and $S_2 = (0, a_2)$ as indicated in the table in Fig. 1.

In the region below the curve $\alpha_C(b)$ there is a retrieval solution R. The value of $\alpha_C(0)$ is $2/\pi = 0.637$ and increases to $\alpha = 0.891$ at $b = 0.405$. At $b \approx 0.484$ there is a steep decrease in α_C with a long tail extending up to $b = 1$. At the upper branch of $\alpha_C(b)$ (solid part in Fig. 1), the solution R goes continuously to the solution S_1, making the latter stable. At the lower branch of $\alpha_C(b)$ (dashed part in Fig. 1) the solutions R and NR coalesce and disappear together. The precise numerical values of this branch of

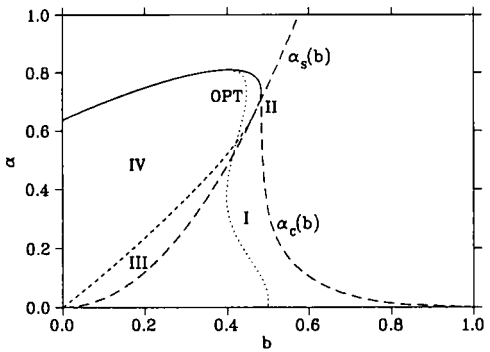

	I	*II*	*III*	*IV*
R	a	a	a	a
NR	s	s	s	-
S_1	-	a	s	s
S_2	-	r	r	s
Z	a	a	a	a

Fig. 1. The (α, b) diagram for the $Q = 3$ network with uniform patterns ($A = 2/3$) at $T = 0$. The curve $\alpha_C(b)$ denotes the boundary of the retrieval region. Below the curve $\alpha_S(b)$ there are no sustained activity solutions. The full line denotes a second-order transition, the dashed line a first-order one. The line *OPT* indicates the network with optimal parameters. The structure I–IV of the retrieval dynamics is explained: *a* denotes an attractor, *s* a saddle point, and *r* a repellor.

$\alpha_c(b)$ depend explicitly on the distribution of the patterns. To fix the ideas we take this distribution to be uniform in all figures.

Concerning the retrieval properties of the neural network it is important to observe that in the retrieval regime, R is never the only attractor in the (m, a) plane. Its basin of attraction is always limited by at least one attractor on the axis $m=0$. Furthermore, at any fixed α, a value of b can be determined where the Hamming distance of R is minimal. The line of these optimal b is indicated by OPT in Fig. 1. Note that this line ends, of course, at the maximal value of $\alpha_c(b)$.

For the $Q=3$ system at $T\neq 0$ explicit formulas for the fixed-point equations are given by (65)–(70) in ref. 1. Formulas analogous to (19), (21), and (22) can be computed from those equations. At sufficiently low temperatures the $T=0$ features of the (α, b) diagram are recovered. It is evident that Z is no longer a solution. It is now, continuously in T, replaced by a new sustained activity solution. Furthermore, as a function of increasing T, $\alpha_c(0)$ slightly increases and then decreases (see also Fig. 3 in ref. 1). At moderate temperatures (e.g., $T=0.10$ in Fig. 2) a more qualitative change has taken place. For each b and α only one sustained activity solution S is left. Below the curve $\alpha_c(b)$ there is a retrieval solution R. If S is a saddle point, R is the only other solution to the fixed-point equations and the transition at $\alpha_c(b)$ is continuous. If S is stable, it is separated from R by yet another solution which is the saddle point NR. At high temperatures the region of instability of S and the retrieval region coincide. Summarising, the introduction of external noise can, depending on α and b, enlarge the basin of attraction of the retrieval solution. However, the quality of retrieval (in terms of Hamming distance) gradually deteriorates as T increases.

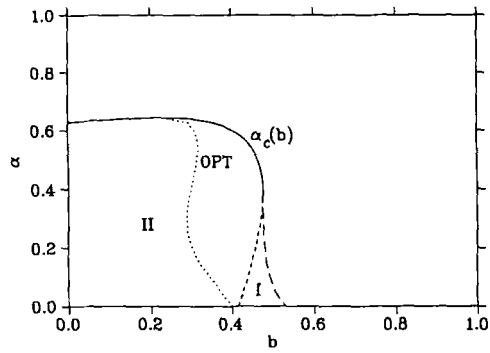

	I	*II*
R	a	a
NR	s	-
S	a	s

Fig. 2. As in Fig. 1, for $T=0.10$. There is no curve $\alpha_s(b)$.

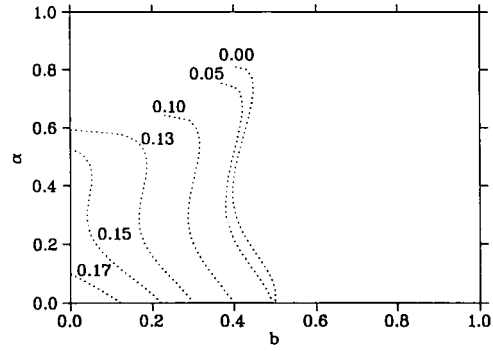

Fig. 3. The evolution of the optimal (α, b) line for the network defined in Fig. 1 as a function of T.

The temperature dependence of the optimal b, i.e., the line OPT, is depicted in Fig. 3. We observe that the line shifts completely to $b=0$ with increasing temperature.

Next we consider the $Q=4$ model. In this case $\mathscr{S}_4=\{-1, -1/3, 1/3, 1\}$. Starting from the general equations (14)–(15) at zero temperature, fixed-point equations can be derived in a straightforward way. For any value of b and α a solution S exists with a given by

$$a=1-\frac{8}{9}\,\mathrm{Erf}\left[\frac{4b/3}{(2\alpha a)^{1/2}}\right] \tag{23}$$

Observe that $a=0$ is not a solution to (23). The stability of S is determined by the sign of the eigenvalues

$$\lambda_1(a)=-1+\frac{4}{3}\frac{1}{(2\pi\alpha a)^{1/2}}\left[\frac{1}{2}+\exp\left(-\frac{(4b/3)^2}{2\alpha a}\right)\right] \tag{24}$$

$$\lambda_2(a)=-1+\frac{8}{9}\frac{4b/3}{(2\pi\alpha a^3)^{1/2}}\exp\left(-\frac{(4b/3)^2}{2\alpha a}\right) \tag{25}$$

For any b and α we find that $\lambda_2(a)<0$. However, for a given b there is a value of α, i.e., $\alpha_C(b)$, where $\lambda_1(a)$ changes sign. For $\alpha<\alpha_C(b)$, $\lambda_1(a)$ is positive such that S is a saddle point. For $\alpha<\alpha_C(b)$ there is at least one retrieval solution. In the region indicated by I in Fig. 4, there are two attracting solutions with $m\neq 0$, denoted by R_1 and R_2. They are separated by a saddle point NR. The solution with the higher overlap m is the real retrieval solution: it is closest in Hamming distance to the embedded

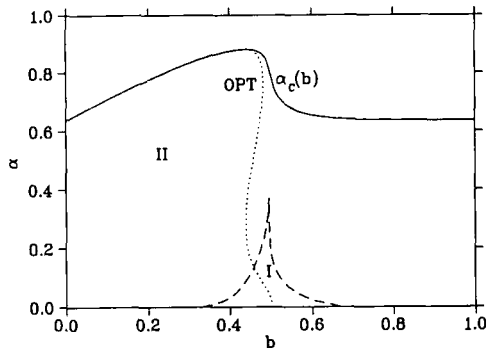

	I	*II*
R_1	a	a
NR	s	-
R_2	a	-
S	s	s

Fig. 4. As in Fig. 1, for the $Q=4$ network with uniform patterns ($A=5/9$) at $T=0$.

pattern. In the limit $b \to \infty$ there exists, for $\alpha < \alpha_C(\infty) = 2/\pi$, a retrieval solution ($m \neq 0$, $a = 1/9$) with m given by

$$m = \frac{1}{6}\,\mathrm{Erf}\left[\frac{3m}{(2\alpha)^{1/2}}\right] + \frac{1}{18}\,\mathrm{Erf}\left[\frac{m}{(2\alpha)^{1/2}}\right] \tag{26}$$

Because the line $\alpha_C(b)$ is the limit of the retrieval region as well as the limit of the instability region for S, it is clear that there is a continuous transition from R to S at this line.

Concerning the retrieval properties of the network, it is important to observe that for appropriately chosen b and α the retrieval solution is the only attractor in the (m, a) plane. However, note that for sufficiently low α the line of optimal b at given α enters region I (see Fig. 4). This implies that in this region the basin of attraction of the retrieval solution with optimal Hamming distance is not the whole (m, a) plane.

For $T \neq 0$ we see that at low temperatures also the $Q=4$ network is a continuously deformed copy of the $T=0$ case. At sufficiently high temperatures the retrieval region becomes bounded in b and the region I disappears. As in the $Q=3$ model, the line of optimal b gradually shifts to $b=0$.

Finally we consider graded-response neurons. At $T=0$ and for an even distribution of the states the fixed-point equations (14)–(15) read

$$m = \frac{1}{2A}\frac{(2\alpha a)^{1/2}}{2b}\left\langle\!\!\left\langle \xi\left[\{X_+(\xi)\,\mathrm{Erf}[X_+(\xi)] - X_-(\xi)\,\mathrm{Erf}[X_-(\xi)]\} + \frac{1}{\sqrt{\pi}}\left(e^{-X_+(\xi)^2} - e^{-X_-(\xi)^2}\right)\right]\right\rangle\!\!\right\rangle \tag{27}$$

$$a = 1 + \frac{1}{2}\frac{\alpha a}{4b^2}\left\langle\!\!\left\langle [1 - 2X_+(\xi)\, X_-(\xi)]\{\mathrm{Erf}[X_+(\xi)] + \mathrm{Erf}[X_-(\xi)]\} \right.\right.$$
$$\left.\left. - \frac{2}{\sqrt{\pi}}[X_+(\xi)\, e^{-X_-(\xi)^2} + X_-(\xi)\, e^{-X_+(\xi)^2}] \right\rangle\!\!\right\rangle \tag{28}$$

where

$$X_\pm(\xi) = \frac{2b \pm m\xi}{(2\alpha a)^{1/2}} \tag{29}$$

Sustained activity solutions satisfy

$$a = 1 - \left(1 - \frac{\alpha a}{4b^2}\right)\mathrm{Erf}\left[\frac{2b}{(2\alpha a)^{1/2}}\right] - \frac{1}{2b}\left(\frac{2\alpha a}{\pi}\right)^{1/2}\exp\left(-\frac{4b^2}{2\alpha a}\right) \tag{30}$$

They have stability eigenvalues

$$\lambda_1(a) = -1 + \frac{1}{2b}\mathrm{Erf}\left[\frac{2b}{(2\alpha a)^{1/2}}\right] \tag{31}$$

$$\lambda_2(a) = -1 + \frac{\alpha}{4b^2}\mathrm{Erf}\left[\frac{2b}{(2\alpha a)^{1/2}}\right] - \frac{1}{2b}\left(\frac{2\alpha}{\pi a}\right)^{1/2}\exp\left(-\frac{4b^2}{2\alpha a}\right) \tag{32}$$

From (31)–(32) we easily derive that Z is an attracting fixed point if both $b > 1/2$ and $\alpha < 4b^2$. An expansion of (30) for small a shows that at $\alpha = \alpha_S(b) = 4b^2$, a nonzero solution bifurcates from the solution $a = 0$, making the latter unstable on the axis $m = 0$ in the (m, a) plane. For the corresponding solution S it is straightforward to show that $\lambda_2(a) < 0$. Consequently, the stability of S depends only on $\lambda_1(a)$. Numerical analysis shows that at fixed b, $\lambda_1(a) > 0$ up to some critical value $\alpha_C(b)$.

Note that all the above conclusions are independent of the distribution of the patterns. To obtain detailed information about the retrieval regime, we assume from now on that the patterns are uniformly distributed on $\mathscr{S}_\infty = [-1, +1]$, which implies $A = 1/3$. Abbreviating $X_\pm(1)$ by $X_\pm$, we find that the fixed-point equations (27)–(28) get the form

$$m = \left(\frac{m}{4b} + \frac{3}{4} - \frac{3\alpha a + 4b^2}{4m^2}\right)\mathrm{Erf}[X_+] + \left(\frac{m}{4b} - \frac{3}{4} + \frac{3\alpha a + 4b^2}{4m^2}\right)\mathrm{Erf}[X_-]$$
$$+ \left(\frac{\alpha a}{2\pi}\right)^{1/2}\left[\left(\frac{1}{2m} + \frac{1}{2b} - \frac{\alpha a + 2b^2}{2bm^2}\right)e^{-X_+^2}\right.$$
$$\left. + \left(\frac{1}{2m} - \frac{1}{2b} + \frac{\alpha a + 2b^2}{2bm^2}\right)e^{-X_-^2}\right] \tag{33}$$

$$a = 1 - \left(\frac{1}{2} + \frac{2b}{3m} - \frac{3\alpha a + m^2}{24b^2}\right) \mathrm{Erf}[X_+]$$
$$- \left(\frac{1}{2} - \frac{2b}{3m} - \frac{3\alpha a + m^2}{24b^2}\right) \mathrm{Erf}[X_-]$$
$$- \left(\frac{\alpha a}{2\pi}\right)^{1/2} \left[\left(\frac{1}{6b} + \frac{2}{3m} - \frac{2\alpha a + m^2}{12mb^2}\right) e^{-X_+^2}\right.$$
$$\left. + \left(\frac{1}{6b} - \frac{2}{3m} + \frac{2\alpha a + m^2}{12mb^2}\right) e^{-X_-^2}\right] \tag{34}$$

For both $b < 1/2$ and $\alpha < \alpha_C(b)$ there is one and only one solution ($m \neq 0$, $a \neq 0$) to (33), (34). The stability properties of S and Z imply that this solution is attracting. Therefore, it is a real retrieval solution, denoted by R. The fact that R attracts the whole (m, a) plane constitutes the main difference with the Q-Ising case (Q finite), where the basin of attraction of the retrieval state is always limited by an attractor on the axis $m = 0$.

Finally, at any fixed α, again a value of b can be determined where the Hamming distance of R is minimal. As can be seen in Fig. 5, the corresponding line OPT lies close to $b = 1/2$. This is connected with the fact that at $\alpha = 0$ the Hamming distance is 0 only for $b = 1/2$.

For $T \neq 0$, the fixed-point equations [recall (16)–(18)] can be composed from the following expressions:

$$\bar{s}(h) = \frac{h}{2b} + \left(\frac{2}{\pi\beta b}\right)^{1/2} \frac{e^{-h_+^2} - e^{-h_-^2}}{\mathrm{Erf}(h_+) + \mathrm{Erf}(h_-)} \tag{35}$$

$$\overline{s^2}(h) = \left(\frac{h}{2b}\right)^2 + \frac{1}{\beta b} + \frac{2}{\sqrt{\pi}\,\beta b} \frac{h_- e^{-h_+^2} - h_+ e^{-h_-^2}}{\mathrm{Erf}(h_+) + \mathrm{Erf}(h_-)} \tag{36}$$

$$h_\pm = \left(\frac{\beta b}{2}\right)^{1/2} \left(\frac{h}{2b} \pm 1\right) \tag{37}$$

The solution Z no longer appears. However, the main characteristics of the network are comparable with the $T = 0$ behavior. There is one solution S which is a saddle point at given b up to some value $\alpha_C(b)$. For $\alpha < \alpha_C(b)$, a retrieval state R exists which attracts the whole (m, a) plane. At $\alpha_C(b)$, R goes continuously to S, making the latter stable (see Fig. 6 at $T = 0.075$). As in the finite-Q models, the line OPT gradually shifts to $b = 0$ with increasing temperature. We remark that the evolution of the retrieval region strongly resembles the results of ref. 3 where the stochasticity has been introduced in a different way.

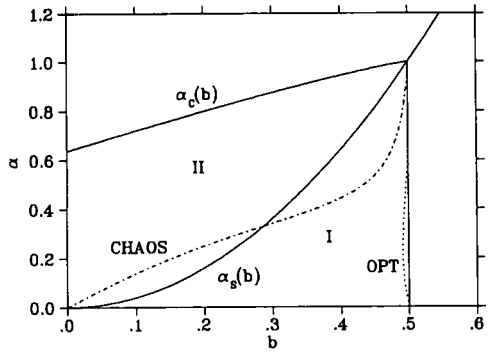

	I	*II*
R	a	a
S	-	s
Z	s	r

Fig. 5. As in Fig. 1, for the piecewise linear network with uniform patterns ($A = 1/3$) at $T = 0$. Above the dynamical transition line *CHAOS* chaotic behavior occurs.

5. MICRODYNAMICS: CHAOTIC PROPERTIES

In this section we estimate the local stability of the trajectories $\boldsymbol{\sigma}(t)$ in the configuration space using the Hamming distance as it was proposed in refs. 13–15. Specifically, we study the time evolution of the Hamming distance between two configurations which are initially close to each other and are both correlated with the embedded pattern. Formally, let us consider two different initial conditions $\boldsymbol{\sigma}(t)$, respectively, $\tilde{\boldsymbol{\sigma}}(t)$, which are collections of i.i.d.r.v. with mean zero and variance a_0, respectively, $\tilde{a}_0$. Furthermore, we assume that they are correlated with the embedded pattern

$$\frac{1}{A}\,\mathrm{E}[\xi_i^\mu \sigma_i(0)] = \delta_{\mu,\nu} m_0, \qquad \frac{1}{A}\,\mathrm{E}[\xi_i^\mu \tilde{\sigma}_i(0)] = \delta_{\mu,\nu} \tilde{m}_0 \tag{38}$$

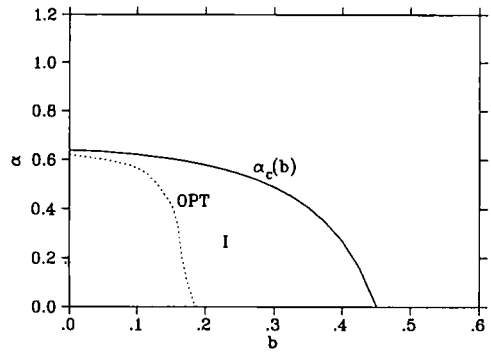

	I
R	a
S	s

Fig. 6. As in Fig. 5, for $T = 0.075$. There is no line *CHAOS*.

whereby in (38) and in the sequel quantities with a tilde correspond to the configuration $\tilde{\boldsymbol{\sigma}}(t)$. Defining the overlap between the two configurations $\boldsymbol{\sigma}(t)$ and $\tilde{\boldsymbol{\sigma}}(t)$ as

$$C_\Lambda(t) \equiv \frac{1}{N} \sum_{i \in \Lambda} \sigma_i(t)\, \tilde{\sigma}_i(t) \tag{39}$$

we find that the LLN yields an initial correlation

$$\mathrm{E}[\sigma_i(0)\, \tilde{\sigma}_j(0)] = \delta_{i,j} C(0) \tag{40}$$

with $C(t) \equiv \lim_{N \to \infty} C_\Lambda(t)$. Now we observe that

$$d_{\mathrm{H}}(\boldsymbol{\sigma}_\Lambda(t), \tilde{\boldsymbol{\sigma}}_\Lambda(t)) = \frac{1}{N} \sum_{i \in \Lambda} [\sigma_i(t) - \tilde{\sigma}_i(t)]^2 = a_\Lambda(t) + \tilde{a}_\Lambda(t) - 2C_\Lambda(t) \tag{41}$$

If we want to obtain information about the Hamming distance $d_{\mathrm{H}}(\boldsymbol{\sigma}(t), \tilde{\boldsymbol{\sigma}}(t))$, it follows immediately that we have to focus on the time evolution of $C(t) = \mathrm{E}[\sigma_i(t)\, \tilde{\sigma}_i(t)]$. This implies that we have to calculate the joint distribution for the dependent random variables $\sigma_i(t)$ and $\tilde{\sigma}_i(t)$.

To this end, reconsider the local field in i [see (13)]

$$h_i(\boldsymbol{\sigma}_{\Lambda \setminus i}(0)) = \xi_i^\nu m_\Lambda^\nu(0) + \frac{1}{(\alpha N^2)^{1/2}} \sum_{\mu \in \mathscr{P} \setminus \nu} \sum_{j \in \Lambda \setminus i} R_{j,\mu}(0) \tag{42}$$

$$R_{j,\mu}(0) \equiv \frac{\sqrt{\alpha}}{A} \xi_i^\mu \xi_j^\mu \sigma_j(0) \tag{43}$$

Because $\{R_{j,\mu}(0)\}$ and similarly $\{\tilde{R}_{j,\mu}(0)\}$ are collections of αN^2 i.i.d.r.v., we have by the two-dimensional CLT that in the limit $N \to \infty$

$$(h_i(\boldsymbol{\sigma}(0)), h_i(\tilde{\boldsymbol{\sigma}}(0))) \overset{\mathscr{D}}{=} (\xi_i^\nu m_0 + R(0), \xi_i^\nu \tilde{m}_0 + \tilde{R}(0)) \tag{44}$$

where now $(R(0), \tilde{R}(0))$ is a couple of correlated centered Gaussians (independent of ξ^ν) with correlation matrix

$$\mathscr{K} = \begin{pmatrix} \alpha a(0) & K(0) \\ K(0) & \alpha \tilde{a}(0) \end{pmatrix} \tag{45}$$

We remark that for correlated Gaussian random variables the joint distribution is indeed completely defined by the correlation matrix.[16] But we also have that

$$\begin{aligned} K(0) &= \frac{\alpha}{A^2} \mathrm{E}[(\xi_i^\mu)^2 (\xi_j^\mu)^2 \sigma_j(0)\, \tilde{\sigma}_j(0)] \\ &= \alpha \mathrm{E}[\sigma_j(0)\, \tilde{\sigma}_j(0)] = \alpha C(0) \end{aligned} \tag{46}$$

This means that in the extremely diluted version of the network, we can immediately conclude, using the LLN in (39) and recalling the dynamics defined by (6),

$$C(t+1)=\int_{\mathbb{R}^2} DH(u,\tilde{u})\ll g(\xi^{\nu}m^{\nu}(t)+u)\ g(\xi^{\nu}\tilde{m}^{\nu}(t)+\tilde{u})\gg \tag{47}$$

$$DH(u,\tilde{u})\equiv\frac{du\,d\tilde{u}}{2\pi\alpha[a(t)\,\tilde{a}(t)-C(t)^2]^{1/2}} \times\exp\left\{-\frac{a(t)\,u^2-2C(t)\,u\tilde{u}+\tilde{a}(t)\,\tilde{u}^2}{2\alpha[a(t)\,\tilde{a}(t)-C(t)^2]}\right\} \tag{48}$$

We now restrict our initial conditions to the case of two configurations with equal overlap $m(t)=\tilde{m}(t)$ and equal activity $a(t)=\tilde{a}(t)$. For convenience we will also write $a\equiv a(t)$, $m\equiv m(t)$, $C\equiv C(t)$, $a'\equiv a(t+1)$, $m'\equiv m(t+1)$, and $C'\equiv C(t+1)$ in the following. With these abbreviations the recursion for the Hamming distance (41) is equivalent to

$$a'-C'=\left\langle\!\!\left\langle\int_{\mathbb{R}} Du\ g^2(\xi^{\nu}m+u)-\int_{\mathbb{R}^2} DH(u,\tilde{u})\ g(\xi^{\nu}m+u)\ g(\xi^{\nu}m+\tilde{u})\right\rangle\!\!\right\rangle \tag{49}$$

To determine the chaotic properties of the trajectories we have to expand (49) for small $a-C$. Note that this equation is still valid for arbitrary $g(\cdot)$. Nevertheless, it is more instructive to perform the expansion first for the finite-Q model with a gain function defined by (6) and with $\mathscr{S}=\mathscr{S}_Q$ [see (7)]. In this case the integration over the variable $\tilde{u}$ in (49) can be carried out, yielding

$$a'-C'=\sum_{l=1}^{Q} s_l\left\langle\!\!\left\langle\int_{A_{l-1}(\xi)}^{A_l(\xi)} Du\left(s_l+\frac{1}{Q-1}\sum_{k=1}^{Q}\operatorname{Erf}\left[\frac{aA_k(\xi)-Cu}{(a^2-C^2)^{1/2}}\right]\right)\right\rangle\!\!\right\rangle \tag{50}$$

where we have introduced

$$A_k(\xi)\equiv\frac{b(s_k+s_{k+1})-\xi m}{(2\alpha a)^{1/2}},\qquad k=0,\ldots,Q \tag{51}$$

In the integrand of the lth term of the first sum in (50) the terms with $k\neq l-1$ and $k\neq l$ can be asymptotically expanded. If $k>l$, the contribution is $+1$; if $k<l-1$, it is -1. The terms with $k=l-1$ or $k=l$ can then be integrated and expanded, yielding an expression of order $(a-C)^{1/2}$, i.e.,

$$a'-C'\approx\frac{4}{\pi(Q-1)}\left(\frac{a-C}{a+C}\right)^{1/2}\frac{1}{Q-1}\sum_{l=1}^{Q-1}\left\langle\!\!\left\langle\exp-\frac{[b(s_l+s_{l+1})-\xi m]^2}{\alpha(a+C)}\right\rangle\!\!\right\rangle \tag{52}$$

The fact that the leading contribution is of order $(a-C)^{1/2}$ means that trajectories that come sufficiently close to each other at some moment in time are strongly repelled after the next time-step. The retrieval and the sustained activity solution of a Q-Ising network (Q finite) thus exhibit chaotic behavior in the way we have defined it. Stated otherwise, the point $C=a$ which corresponds to the case $\boldsymbol{\sigma}=\tilde{\boldsymbol{\sigma}}$ is not stable. Because in (52) the coefficient of $(a-C)^{1/2}$ is effectively proportional to Q^{-1}, we can expect that in the limit $Q\to\infty$ [i.e., the piecewise linear gain function (8)] the leading term will no longer be of order $(a-C)^{1/2}$. A more careful computation starting again from (49) shows that the first term in the expansion is indeed linear in $a-C$,

$$a'-C'\approx\frac{\alpha}{4b^2}\left\langle\!\!\left\langle \operatorname{Erf}\left[\frac{2b+\xi m}{(2\alpha a)^{1/2}}\right]\right\rangle\!\!\right\rangle (a-C) \tag{53}$$

Consequently, the coefficient of $a-C$ in (53) has to be analyzed. In the retrieval regime, and using the fixed-point values of m and a [see (33) and (34)], we find that for $\alpha\to 0$ the behavior is not chaotic. However, for any b there is an α at which the coefficient becomes greater than unity, which means that the chaotic regime sets in. The corresponding line is depicted in Fig. 5. It is interesting to note that in the sustained activity regime (i.e., the case $m=0$) the behavior is always chaotic.

It is generally known that in a finite-dimensional dynamical system the existence of a positive Lyapunov exponent implies that the spectrum of the autocorrelation function is continuous.[8] Furthermore, this autocorrelation exponentially decays with an exponent equal to the largest Lyapunov exponent. Here, too, we can make a connection between the behavior of the correlation (39) between two configurations and the behavior of the autocorrelation defined as

$$\chi(t+1,t'+1)\equiv \mathrm{E}[\sigma_i(t+1)\,\sigma_i(t'+1)] \tag{54}$$

where $\{\sigma_i(0)\}$ is again a collection of i.i.d.r.v. correlated with the embedded pattern. It is sufficient to observe that a dynamical functional approach in complete analogy with the binary Ising case (see, e.g., ref. 19 and the references therein) results in the following recursion for the autocorrelation $\chi(t+1,t'+1)$:

$$\chi(t+1,t'+1)=\int_{\mathbb{R}^2} DH(u,v)\langle\!\langle\, g(\xi^\nu m^\nu(t)+u)\; g(\xi^\nu m^\nu(t')+v)\,\rangle\!\rangle \tag{55}$$

$$DH(u,v)\equiv\frac{du\,dv}{2\pi\alpha[a(t)\,a(t')-\chi(t,t')^2]^{1/2}} \times\exp\left\{-\frac{a(t)\,u^2-2\chi(t,t')\,uv+a(t')\,v^2}{2\alpha[a(t)\,a(t')-\chi(t,t')^2]}\right\} \tag{56}$$

From (47)–(48) on the one hand and (55)–(56) on the other it is obvious, recalling (14), that the chaotic properties of the dynamics can also be investigated starting from the recursion for

$$d_{\mathrm{H}}(\boldsymbol{\sigma}(t), \boldsymbol{\sigma}(t')) = a(t) + a(t') - 2\chi(t, t') \tag{57}$$

Conclusions can be drawn from the evolution of this equation parallel to those arrived at by considering the evolution of (41).

We have already observed that the chaotic behavior of the trajectories in the configuration space in fact means that the fixed point $C = a$ in (47)–(48) is not stable. More precisely, we find that for $\alpha \to 0$ the stable solution to this equation deviates from the fixed-point value of the activity a as

$$C \approx a - \frac{8}{\pi^2 a (Q-1)^4} \left\{ \sum_{l=1}^{Q-1} \left\langle\!\!\left\langle \exp\left(- \frac{[b(s_l + s_{l+1}) - \xi m]^2}{2\alpha a} \right) \right\rangle\!\!\right\rangle \right\}^2 \tag{58}$$

We remark that an analogous expression can immediately be written down for the limiting value of the autocorrelation function $\chi \equiv \lim_{t,t' \to \infty} \chi(t + t', t')$.

The result (58) constitutes the generalization of a well-known formula for networks of binary neurons [see, e.g., Eq. (6.63) in ref. 19].

6. CONCLUDING REMARKS

In this paper we have derived the evolution equations governing the parallel dynamics at arbitrary temperatures for extremely diluted Q-state Ising and graded-response networks with general input–output functions.

We have studied in detail the macroscopic structure of the retrieval region in the case of steplike and piecewise linear gain functions. In particular dynamical capacity–gain diagrams have been analyzed as a function of the temperature for $Q = 3$, $Q = 4$, and in the limit $Q \to \infty$. The properties of the zero solution, the sustained activity solutions, and the retrieval solutions have been determined. The line of optimal Hamming distance in the capacity–gain plane has been calculated. It is found that in the case of analog neurons the retrieval solution attracts the whole overlap–activity plane, in contrast to the case of Q-state neurons, where its basin of attraction is always limited.

Some microscopic properties of the networks considered as discrete dynamical systems have also been investigated. Specifically the Hamming distance between two neighboring trajectories has been used as a measure for the local instability and complexity of the attractors for the parallel

dynamics. To this end we have fixed two initial configurations by choosing the nonzero projection on the embedded pattern, the activity, and the mutual projection. For the finite-Q network it is found that two arbitrarily close configurations chosen in this way always repel each other, implying chaotic behavior, even in the retrieval regime. For the graded-response network, however, there exists a transition line in the capacity–gain plane below which no such chaotic behavior occurs. We remark that for a general Q-Ising network ($Q > 2$) the constraints to fix the initial configurations are not exhaustive in the sense that there is more than one distribution of initial conditions which satisfy them. In fact here we have used a uniform distribution, which is conserved by the dynamics. Consequently, the distance between two distributions of random initial configurations could be used as a more general measure for the common evolution of these configurations.

ACKNOWLEDGMENTS

This work has been supported in part by the Research Fund of the K.U. Leuven (grant OT/91/13). One of us (D.B.) thanks the Belgian National Fund for Scientific Research for support as a Research Director.

REFERENCES

1. D. Bollé, B. Vinck, and V. A. Zagrebnov, *J. Stat. Phys.* **70**:1099 (1993).
2. H. Rieger, in *Statistical Mechanics of Neural Networks*, L. Garrido, ed. (Springer, Berlin, 1990), p. 33.
3. S. Mertens, *J. Phys. A* **24**:337 (1991).
4. D. Gandolfo, J. Ruiz, and V. A. Zagrebnov, On the parallel dynamics of the diluted clock neural network, Preprint Marseille CPT-92/P.2728.
5. J. Jedrzejewski and A. Komoda, *Europhys. Lett.* **18**:275 (1992).
6. E. Gardner, *J. Phys. A* **19**:L1047 (1986).
7. C. Newman, *Neural Networks* 1:223 (1988).
8. G. M. Zaslavsky, R. Z. Sagdeev, D. A. Usikov, and A. A. Chernikov, *Weak Chaos and Quasi-regular Patterns* (Cambridge University Press, Cambridge, 1991).
9. H. Sompolinsky, A. Crisanti, and H. J. Sommers, *Phys. Rev. Lett.* **61**:259 (1988).
10. B. Tirozzi and M. Tsodyks, *Europhys. Lett.* **14**:727 (1991).
11. L. Molgedey, J. Schuchardt, and H. G. Schuster, *Phys. Rev. Lett.* **26**:3717 (1992).
12. M. Bauer and W. Martienssen, *J. Phys. A* **24**:4557 (1991).
13. B. Derrida, E. Gardner, and A. Zippelius, *Europhys. Lett.* **4**:167 (1987).
14. B. Derrida, *J. Phys. A* **20**:L721 (1987).
15. B. Derrida and R. Meir, *Phys. Rev. A* **38**:3116 (1988).
16. A. N. Shiryaev, *Probability* (Springer-Verlag, Berlin, 1991).
17. L. Wang and J. Ross, *Phys. Rev. A* **44**:R2259 (1991).
18. H. Rieger, *J. Phys. A* **23**:L1273 (1990).
19. R. Kree and A. Zippelius, in *Models of Neural Networks*, E. Domany, J. L. van Hemmen, and K. Schulten, eds. (Springer-Verlag, Berlin 1991), p. 193.